

## Nonadiabatic alignment of van der Waals–force-bound argon dimers by femtosecond laser pulses

J. Wu,<sup>1,2</sup> A. Vredenburg,<sup>1</sup> B. Ulrich,<sup>1</sup> L. Ph. H. Schmidt,<sup>1</sup> M. Meckel,<sup>1</sup> S. Voss,<sup>1</sup> H. Sann,<sup>1</sup> H. Kim,<sup>1</sup> T. Jahnke,<sup>1</sup> and R. Dörner<sup>1,\*</sup>

<sup>1</sup>*Institut für Kernphysik, Goethe Universität, Max-von-Laue-Strasse 1, D-60438 Frankfurt, Germany*

<sup>2</sup>*State Key Laboratory of Precision Spectroscopy, East China Normal University, Shanghai 200062, China*

(Received 23 February 2011; published 23 June 2011)

We demonstrated that the weak van der Waals–force-bound argon dimer can be nonadiabatically aligned by nonresonant femtosecond laser pulses, showing periodic alignment and anti-alignment revivals after the extinction of the laser pulse. Based on the measured nonadiabatic alignment trace, the rotational constant of the argon dimer ground state is determined to be  $B_0 = 0.05756 \pm 0.00004 \text{ cm}^{-1}$ . Noticeable alignment dependence of frustrated tunneling ionization and bond-softening induced dissociation of the argon dimer are observed.

DOI: [10.1103/PhysRevA.83.061403](https://doi.org/10.1103/PhysRevA.83.061403)

PACS number(s): 32.80.Rm, 33.80.–b, 33.15.Bh, 42.65.Re

Moderately intense laser pulses can efficiently align molecules, i.e., confine the molecular axes to axes fixed in space. In the nonadiabatic limit where the pulse duration is much smaller than the inherent rotational period a rotational wave packet is induced in each molecule by stimulated Raman transitions. The quantum beats between the states leads to field-free alignment and anti-alignment revivals of the nonadiabatically aligned molecular ensemble after the laser pulse [1]. In the past, the nonadiabatic molecular alignment has attracted a lot of interest for its extensive range of applications such as tomographic imaging of molecular orbitals [2], laser induced electron diffraction [3], quantum interference in high-harmonic generation [4], and ultrashort laser pulse manipulation and characterization [5,6]. The degree of molecular alignment could be increased by using a train of sequential pulses [7] or shaped ultrashort pulses [8]. Three-dimensional alignment of complex molecules were created by using elliptically polarized laser pulses [9,10]. Recently, adiabatic alignments of rare-gas dimers with nanosecond pulses were demonstrated to characterize the polarizability anisotropies [11]. Nonadiabatic alignment of molecular cluster was achieved to extract the rotational constant [12], which requires a molecular cluster to possess a long-lived excited state and thus cannot be applied to the rare-gas dimer.

In this Rapid Communication, we demonstrate that the weak van der Waals–force-bound rare-gas argon dimer ( $\text{Ar}_2$ ) can be nonadiabatically aligned by using nonresonant femtosecond laser pulses. The field-free alignment and anti-alignment revival structures were measured up to  $\sim 1$  ns after the nonadiabatic excitation of the laser pulse without noticeable decay of alignment contrast and change of the shape, indicating a well-preserved coherence of the rotational wave packets. We extracted the ground state rotational constant from the nonadiabatic alignment trace and determine it to be  $B_0 = 0.05756 \pm 0.00004 \text{ cm}^{-1}$ . The alignment dependence of the bond-softening induced dissociation and frustrated tunneling ionization of argon dimer are observed.

The  $\text{Ar}_2$  bound by the weak van der Waals force ( $\sim 12.3 \text{ meV}$  or  $99.2 \text{ cm}^{-1}$ ) at a large internuclear distance ( $R_e \sim 7.1 \text{ a.u.}$ ) [13,14] shows features of both atoms and molecules

and has attracted growing interest for its interaction with ions [15], synchrotron radiation [16] and strong laser fields [17,18]. Rare-gas dimers with their extraordinary large internuclear distance and the absence of real delocalized molecular orbitals have a unique combination of atomic structure and energetics with an additional axis as the only molecular feature. Analogous to the covalently bound molecules [2–6], the possibility to nonadiabatically align the rare-gas dimers promise a rich set of interesting applications in various fields.

Experimentally, a femtosecond laser pulse with 35 fs duration centered at 790 nm produced from a multipass amplifier Ti:sapphire laser system (KMLabs Dragon) was split into two: an aligning “pump” and an ionizing “probe”. The pump part of the beam was sent to a traveling-wave optical parametric amplifier superfluorescence (TOPAS) to generate infrared pulses at 1400 nm and used to nonadiabatically align the  $\text{Ar}_2$ . Less multiphoton ionization probability is expected for the long wavelength laser pulse, which will therefore benefit the alignment. The ionizing probe pulse at 790 nm wavelength was time delayed with respect to the pump by means of a computerized translation stage, which is then used to reconstruct the alignment revivals by imaging the Coulomb explosion (CE) channels. After a combing mirror, the pump and probe pulses were collinearly sent into a standard cold target recoil ion momentum spectroscopy (COLTRIMS) setup [19,20] and focused by a parabolic reflection mirror with a focal length of 7.5 cm onto a supersonic gas jet. The probe pulse was 2 times expanded in beam diameter by a telescope to produce a smaller focusing volume at the molecular beam as compared to the pump pulse. As shown in the inset of Fig. 1(a), the pump pulse was linearly polarized along the time of flight direction of the ion spectrometer ( $z$  direction of the laboratory frame) and the probe pulse was set to be circularly polarized (in the  $y$ - $z$  plane of the laboratory frame) by passing through a quarter wave plate. The  $\text{Ar}_2$  supersonic jet source was the same as described in detail in Ref. [17]. A fraction of about 1–2% dimers were produced with respect to the atomic monomer. The ionic fragments created by the laser pulse were projected to the position and time sensitive micro channel plate detector [21] at the end of the spectrometer. The 3D momentum vectors were reconstructed from the measured time-of-flight and the position of impact on the detector for each particle during an off-line analysis. The peak intensities

\*doerner@atom.uni-frankfurt.de

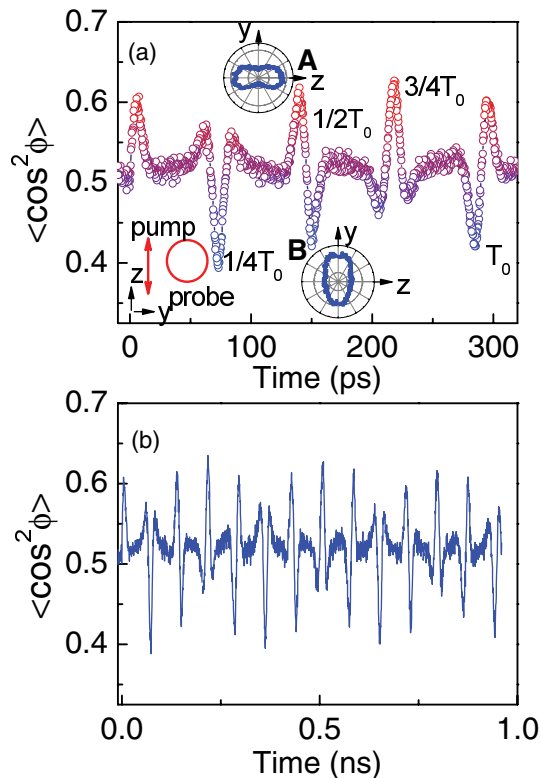


FIG. 1. (Color online) The measured field-free alignment of argon dimer for (a) one and (b) three revival periods. The insets show the typical angular distributions of the argon dimers for the alignment (labeled as A) and anti-alignment (labeled as B) cases around the half-revival period. The pump pulse is polarized in the  $z$  direction and the probe pulse is circularly polarized in the  $y$ - $z$  plane.

of the pump and probe pulses at the gas jet were estimated to be  $\sim 8 \times 10^{13}$  and  $1 \times 10^{15}$  W/cm<sup>2</sup>, respectively. No ionization of Ar<sub>2</sub> was observed from the pump pulse without probe.

Figure 1(a) shows the measured field-free revival structure of the nonadiabatically aligned Ar<sub>2</sub>. The dimers are first aligned along the polarization of the pump pulse at a time delay of  $\sim 5.66$  ps and then clearly show the anti-alignment and alignment structures at the fractional and full revival periods. The alignment degree is characterized by  $\langle \cos^2 \Phi \rangle$ , where  $\Phi$  is the angle between the dimer axis and pump field direction in the circular polarization plane of the probe pulse. The average term of  $\langle \cos^2 \Phi \rangle = 0.5$  corresponds to the random orientation since isotropic ionization dynamics is expected in the polarization plane of the circularly polarized probe pulse. The alignment and anti-alignment of the dimers result in values larger and smaller than 0.5, respectively [22,23]. Here, the double ionization induced CE channel  $\text{Ar}_2^{2+} \rightarrow \text{Ar}^+ + \text{Ar}^+$  [labeled as Ar(1,1)] in the circular polarization plane of the probe pulse was used to reconstruct the time-dependent revival structures of the nonadiabatically aligned dimer. For this symmetric breakup, no handedness dependence is expected [22]. The events of the Ar(1,1) channel were clearly selected from the measured data by using the two-ion coincidence condition, i.e., the momentum conservation of the two ionic fragments [17]. The angular distributions of the Ar<sup>+</sup> from the Ar(1,1) channel for the alignment (labeled with A) and anti-alignment (labeled

with B) revivals are plotted as insets. They clearly show the alignment and anti-alignment of the Ar<sub>2</sub> with the dimer axis aligned in parallel and orthogonal to the pump pulse polarization, respectively.

The full revival period was extracted to be  $T_{\text{rev}} \sim 289.74 \pm 0.19$  ps, leading to a rotational constant  $B_0 = 1/(2T_{\text{rev}} c)$  of  $0.05756 \pm 0.00004$  cm<sup>-1</sup>, where  $c$  is the velocity of light. This value of the rotational constant lies in the range of the reported ones (ranging from 0.05708 to 0.05787 cm<sup>-1</sup>) obtained with different methods (e.g., spectroscopy) [14,24]. However, this slight difference of the rotational constant  $B_0$  will lead to a significant change of the revival period  $T_{\text{rev}}$  from 292.18 to 288.20 ps, which can be clearly distinguished from our measurement with femtosecond time resolution.

The rotational state populations can be obtained by Fourier transforming the measured nonadiabatic alignment trace into the frequency domain. Since the molecular alignment is based on multiple Raman transitions, the rotational quantum number  $J$  can be obtained from the beating frequency  $\Delta\omega_{J,J+2} = \omega_{J+2} - \omega_J = 2\pi c B_0(4J+6)$  [22]. Figure 2(a) shows the relative population of the rotational states obtained by Fourier transforming the measured revival structures of Fig. 1(a). In our experiments, most of the dimers were found in the  $J = 2$  and  $J = 4$  rotational states, and only the even rotational states were populated. This agrees with the fact that, for Ar<sub>2</sub> with each atomic nuclear spin of zero and ground state of  $X^1\Sigma_g^+$ , the nuclear spin statistical weight of the odd and even rotational

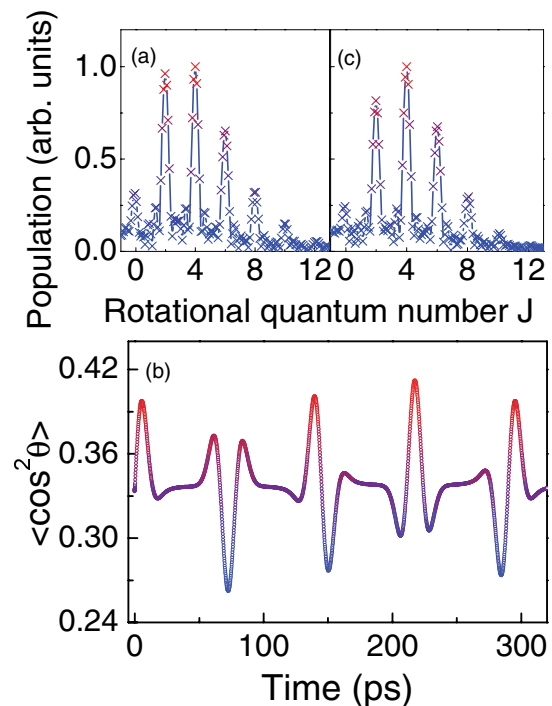


FIG. 2. (Color online) (a) The rotational state populations of the argon dimer obtained by Fourier transforming the measured time-dependent revival structures into the frequency domain. (b) The simulated revival structure of the argon dimer, and (c) the corresponding rotational state populations. Here, since the angular distribution is averaged over the  $\theta$  angle with respect to the pump pulse polarization rather than the  $\Phi$  angle, the isotropic orientation accounts for  $\langle \cos^2 \theta \rangle = 1/3$ .

states are  $g_{J\text{odd}} = 0$  and  $g_{J\text{even}} = 1$ , respectively. As shown in Fig. 1(b), in our experiment, the rotational revival structures can be measured up to  $\sim 1$  ns without noticeable decrease of the strength and change of the shape. These indicate a well preserved coherence of the nonadiabatically excited rotational wave packets and negligible centrifugal distortion [25]. Meanwhile, it indicates that the nonadiabatic alignment in our experiment is mainly contributed by the ground state of the  $\text{Ar}_2$  rather than its strong coupling with excited states. Noticeable change of the revival structure would be expected if there are a certain amount of excited states for their different rotational constants [12]. The negligible contribution of the excited states also agrees with the low temperature of the  $\text{Ar}_2$  beam in our experiment.

By assuming a quantum mechanical rigid rotor for the rotation of the dimer, Fig. 2(b) shows the simulated revival structure of the nonadiabatic alignment of the  $\text{Ar}_2$  by solving the time-dependent Schrödinger equation  $i\hbar\partial|\psi\rangle/\partial t = H_{\text{eff}}|\psi\rangle$  for the rotational states and thermally averaging over their initial Boltzmann distribution [26]. Here,  $H_{\text{eff}} = B_0J(J+1) - 0.25\Delta\alpha E^2(t)\cos^2\theta$  is the effective Hamiltonian,  $\Delta\alpha$  is the polarizability difference between the components parallel and perpendicular to the dimer axis,  $E(t)$  is the envelope of the laser pulse,  $\theta$  is the angle between the dimer axis and the pump pulse polarization. The peak intensity of the pump pulse centered at 1400 nm with a pulse duration of 35 fs was set to be  $8 \times 10^{13}$  W/cm<sup>2</sup>. The polarizability difference of the  $\text{Ar}_2$  was set to  $\Delta\alpha = 2.21$  a.u. [27], which is about 0.2 of the polarizability of the Ar atom. The initial rotational temperature of the dimer was set to be  $T_{\text{rot}} = 2$  K, which showed a good agreement with the experimental measurement of the arriving time of the first alignment maximum after the excitation pulse as well as the other revivals. The first alignment maximum arrives earlier if the initial temperature is increased which is much more sensitive as compared with the change of the laser intensity. This was used to adjust the initial rotational temperature in the simulation. The rotational temperature of the molecular beam is very close to the translation temperature [22,28], which can be experimentally estimated from  $T_{\text{trans}} = \Delta p^2/[4\ln(4)k_B m]$ . Here,  $k_B$  is the Boltzmann constant,  $\Delta p$  and  $m$  are the full-width at half-maximum (FWHM) of the momentum distribution (in the jet direction) and mass of the singly ionized dimer, respectively. In our experiment we measure a momentum width in the jet direction of  $\Delta p \sim 3.5$  a.u. of  $\text{Ar}_2^+$  ions created by a laser pulse linearly polarized along  $z$  direction (orthogonally to the gas jet). This results in an upper limit of the temperature of the  $\text{Ar}_2$  in the supersonic gas jet of  $\sim 4.7$  K. The corresponding rotational state populations of the simulated molecular alignment revivals are shown in Fig. 2(c), which also shows reasonable agreement with the experimental results [see Fig. 2(a)].

For the data discussed so far we have used circularly polarized light for the probe pulse to reduce an influence of a possible polarization dependence of the probe ionization step on the measured angular distributions. In the following, as shown in the inset of Fig. 3(c), we switch to a probe pulse that is linearly polarized and oriented parallel to the pump pulse, i.e., in the direction of alignment. Exposed to the intense probe pulse, the neutral dimers are multiply ionized by simultaneously absorbing several photons, leading to direct

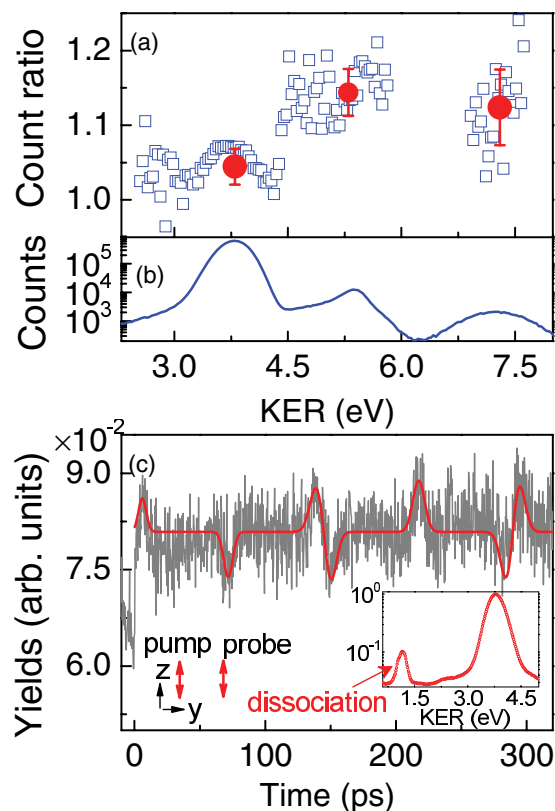


FIG. 3. (Color online) (a) The count ratio between the alignment and anti-alignment cases for the  $\text{Ar}(1,1)$  channel. The circular (red) spots show the corresponding mean value. The two higher KER peaks show significantly stronger alignment dependences than the low energy peak. (b) The KER distribution of the  $\text{Ar}(1,1)$  channel for linearly polarized light. (c) The alignment dependent yield of the bond-softening induced dissociation of the argon dimer (peaked at  $\sim 1.17$  eV as shown in the inset without coincident condition). The red-solid curve shows the multiple Gaussian peaks fit of the measured data. Both the pump and probe pulses are linearly polarized along the  $z$  direction.

CE of the charged nuclei. The production of  $\text{Ar}^+ + \text{Ar}^+$  by linearly polarized light has been shown [17,18] to proceed through three different double ionization mechanisms leading to three different peaks in the kinetic energy release (KER) distribution at 3.8, 5.3 and 7.3 eV [see Fig. 3(b)]. The main peak at 3.8 eV is the same as in the case of circularly polarized light. It results from two site double ionization. The peak at 7.3 eV is only present for linearly polarized light. As 7.3 eV is close to the KER found for a  $\text{Ar}^{2+} + \text{Ar}^+$  pair of 7.5 eV, this contribution in the  $\text{Ar}^+ + \text{Ar}^+$  channel is believed to be due to frustrated triple ionization [29]. In this case one of the three electrons is recaptured into a Rydberg state upon its return to the parent ion in the linearly polarized laser field. The potential energy curves of these states are in the relevant region very close to the one for  $\text{Ar}^{2+} + \text{Ar}^+$ . It has been speculated [17,18] that the intermediate peak at 5.3 eV is due to double ionization with excitation to an excited state of the  $\text{Ar}_2^{2+}$  which is steeper than the ground state. Figure 3(a) shows the alignment dependence of these three KER peaks by comparing the ionization rate of the dimers when the time

delay of the probe pulse is tuned to match the alignment and anti-alignment revivals of the pre-aligned  $\text{Ar}_2$  [as labeled with A and B in Fig. 1(a)]. The two higher KER peaks show significantly stronger alignment dependences than the low energy peak. This is in agreement with the expectations for frustrated triple ionization, as the freeing of the third electron can be expected to be strongly favored when the molecule is oriented parallel to the polarization. The alignment dependent ionization has been observed in covalently bound molecules [22,30], while not in the frustrated tunneling ionization of the van der Waals–force-bound rare-gas dimers. The recent study of the CE of the  $\text{Xe}_2$  showed negligible dependence on the pulse duration with respect to the  $\text{I}_2$  [31], which might also relate to the time-delayed response of the alignment of  $\text{Xe}_2$  (similar to the  $\text{Ar}_2$ ).

In addition to the above-mentioned three CE peaks, as shown in the inset of Fig. 3(c), we also observe another KER peak located at  $\sim 1.17$  eV for the ionic fragment  $\text{Ar}^+$  alone. It disappears if the two-ion coincidence condition is applied. We attribute this low KER peak to the dissociation of the singly ionized dimer  $\text{Ar}_2^+ \rightarrow \text{Ar}^+ + \text{Ar}$  [labeled as  $\text{Ar}(1,0)$ ] through the one-photon bond-softening process, where the neutral Ar fragment cannot be detected in our experiment. Similar to the well studied  $\text{H}_2^+$  [32], this bond-softening dissociation channel can proceed through one-photon coupling between the  $\text{I}(1/2)u$  and  $\text{II}(1/2)g$  states of  $\text{Ar}_2^+$ . Based on the potential curves of these  $\text{I}(1/2)u$  and  $\text{II}(1/2)g$  states [33], we estimated the KER of the fragments  $\text{Ar}^+ + \text{Ar}$  to be  $\sim 1.18$  eV for the probe pulse centered at 790 nm in good agreement with our experimental measurement. Since this

one-photon coupling between the  $\text{I}(1/2)u$  and  $\text{II}(1/2)g$  states is the strongest when the  $\text{Ar}_2$  is aligned along the field, an alignment dependent yield of the  $\text{Ar}(1,0)$  dissociation is therefore expected. Our experimental result for a probe pulse linearly polarized parallel to the pump [Fig. 3(c)] nicely confirms this expectation. The  $\text{Ar}(1,0)$  yield (normalized to the  $\text{Ar}^+$  from the single ionization of atomic Ar) closely follows the field-free revivals of the nonadiabatically aligned  $\text{Ar}_2$ . The increase of the ion yield for the positive time delay (with respect to the negative time delay) indicates the promotion of the bond-softening induced dissociation by the nonadiabatic excitation of the pump pulse. Interestingly, the  $\text{Ar}_2$  bound by weak van der Waals–force behaviors as the covalently bound molecule (e.g.,  $\text{H}_2$ ), clearly showing the bound-softening induced dissociation and alignment dependence.

In summary, we have demonstrated the first nonadiabatic alignment of the van der Waals–force-bound argon dimer by using femtosecond laser pulse. The ground state rotational constant was determined to be  $B_0 = 0.05756 \pm 0.00004 \text{ cm}^{-1}$  from the measured nonadiabatic alignment trace with femtosecond time resolution. The coherence of the nonadiabatically excited rotational wave packets is well preserved for a long time. Noticeable alignment dependence of the frustrated tunneling ionization and bond-softening induced dissociation of the argon dimer were observed.

J.W. acknowledges support by the Alexander von Humboldt Foundation. Support by a Koselleck Project of the Deutsche Forschungsgemeinschaft is acknowledged.

- 
- [1] T. Seideman and E. Hamilton, *Adv. At. Mol. Opt. Phys.* **52**, 289 (2005).
- [2] J. Itatani *et al.*, *Nature (London)* **432**, 867 (2004).
- [3] M. Meckel *et al.*, *Science* **320**, 1478 (2008).
- [4] T. Kanai *et al.*, *Nature (London)* **435**, 470 (2005).
- [5] R. Bartels *et al.*, *Phys. Rev. Lett.* **88**, 013903 (2001); S. Varma, Y. H. Chen, and H. M. Milchberg, *ibid.* **101**, 205001 (2008); J. Wu, H. Cai, Y. Peng, and H. Zeng, *Phys. Rev. A* **79**, 041404(R) (2009).
- [6] P. Lu *et al.*, *Appl. Phys. Lett.* **97**, 061101 (2010); J. Liu *et al.*, *Opt. Express* **19**, 40 (2011).
- [7] C. Z. Bisgaard, M.D. Poulsen, E. Peronne, S. S. Viftrup, and H. Stapelfeldt, *Phys. Rev. Lett.* **92**, 173004 (2004).
- [8] T. Suzuki, Y. Sugawara, S. Minemoto, and H. Sakai, *Phys. Rev. Lett.* **100**, 033603 (2008).
- [9] J. J. Larsen, K. Hald, N. Bjerre, H. Stapelfeldt, and T. Seideman, *Phys. Rev. Lett.* **85**, 2470 (2000).
- [10] H. Tanji, S. Minemoto, and H. Sakai, *Phys. Rev. A* **72**, 063401 (2005).
- [11] S. Minemoto, H. Tanji, and H. Sakai, *J. Chem. Phys.* **119**, 7737 (2003).
- [12] C. Riehn, *Chem. Phys.* **283**, 297 (2002); M. Kuniski *et al.*, *Phys. Chem. Chem. Phys.* **12**, 72 (2010).
- [13] F. M. Tao and Y. K. Pan, *Mol. Phys.* **81**, 507 (1994).
- [14] K. Patkowski *et al.*, *Mol. Phys.* **103**, 2031 (2005), and references therein.
- [15] J. Matsumoto *et al.*, *Phys. Rev. Lett.* **105**, 263202 (2010).
- [16] Y. Morishita *et al.*, *Phys. Rev. Lett.* **96**, 243402 (2006).
- [17] B. Ulrich *et al.*, *Phys. Rev. A* **82**, 013412 (2010).
- [18] B. Manschwetus *et al.*, *Phys. Rev. A* **82**, 013413 (2010).
- [19] J. Ullrich *et al.*, *J. Phys. B* **30**, 2917 (1997).
- [20] R. Dörner *et al.*, *Phys. Rep.* **330**, 95 (2000).
- [21] O. Jagutzki *et al.*, *Nucl. Instrum. Methods Phys. Res. A* **477**, 244 (2002).
- [22] I. V. Litvinyuk *et al.*, *Phys. Rev. Lett.* **90**, 233003 (2003); P. W. Dooley *et al.*, *Phys. Rev. A* **68**, 023406 (2003).
- [23] A. Goban, S. Minemoto, and H. Sakai, *Phys. Rev. Lett.* **101**, 013001 (2008).
- [24] NIST chemistry web book, [<http://webbook.nist.gov/chemistry>].
- [25] E. Hamilton *et al.*, *Phys. Rev. A* **72**, 043402 (2005).
- [26] J. Ortigoso *et al.*, *J. Chem. Phys.* **110**, 3870 (1999); J. Wu, H. Cai, A. Couairon, and H. Zeng, *Phys. Rev. A* **79**, 063812 (2009).
- [27] H. P. Godfried and I. F. Silvera, *Phys. Rev. A* **27**, 3008 (1983).
- [28] M. Hillenkamp *et al.*, *J. Chem. Phys.* **118**, 8699 (2003).
- [29] T. Nubbemeyer, K. Gorling, A. Saenz, U. Eichmann, and W. Sandner, *Phys. Rev. Lett.* **101**, 233001 (2008); B. Manschwetus *et al.*, *ibid.* **102**, 113002 (2009).
- [30] H. Stapelfeldt, *Eur. Phys. J. D* **26**, 15 (2003).
- [31] S. Minemoto and H. Sakai, *Phys. Rev. A* **75**, 033413 (2007).
- [32] A. Giusti-Suzor *et al.*, *J. Phys. B* **28**, 309 (1995), and references therein.
- [33] T. K. Ha *et al.*, *Mol. Phys.* **101**, 827 (2003).